Malaysian Journal of Civil Engineering 27(3):337-355 (2015)

GUST RESPONSE ANALYSIS OF OVERHEAD TRANSMISSION LINES FOR INTERPRETATION OF WIND-INDUCED VIBRATIONS MEASURED IN THE FIELD

Md. Robiul Awall[1]*, Hiroki Yamaguchi[2] & Tasnuva Humyra[3]

[1] *Department of Civil Engineering, Rajshahi University of Engg. & Technology, Rajshahi, Bangladesh*
[2] *Graduate School of Science and Engineering, Saitama University, Japan*
[3] *Department of Civil Engineering, Rajshahi Science & Technology University, Natore, Bangladesh*

*Corresponding Author: *robi95@gmail.com*

Abstract: Several accidents occurred in bundle conductor overhead transmission lines due to large amplitude wind induced vibrations. In evaluating possible causes of these accidents and to develop appropriate counter measures, it is important to have a clear interpretation of the nature of vibrations which actually occurs in the field. This study is carried out to interpret large amplitude field measured wind induced vibrations based on gust response analysis of overhead transmission lines. Time average characteristics of field measured wind-induced vibrations have been discussed based on spectral analysis and time series acceleration. Eigenvalue analysis results of developed three dimensional finite element (FE) model of transmission lines has been discussed with dominant frequency of field measured response spectrum. Wind force has been modeled based on field measured characteristics of wind. Gust response of transmission lines has been evaluated by using developed finite element model of transmission lines and discussed with field measured vibrations. Results from field measured data analysis and eigenvalue analysis showed that cause of large amplitude vertical vibration does not happen due to resonance and galloping of transmission line-A. In case of transmission line-B, some events are found due to resonance and others events have a possibility of galloping as well as gust responses. Random peaks have been observed in time series acceleration which implies impulsive response and well confirmed with numerically obtained gust responses by using FE analysis. Suspension span are more prone in torsional response which are well confirmed with numerical results.

Keywords: *Overhead transmission line, gust response, finite element method, eigenvalue analysis, resonance, torsional response*

1.0 Introduction

In modern days, reliable electricity supply is primary importance for the industry as well as for the private consumer. The overhead transmission line systems exposed on the open air climate and undergo a variety of severe events leading to the failure of the power transmission. All over the world including Japan, several accidents happen in transmission line due to large amplitude wind induced vibration. The interruption of electrical service occurs due to failure of transmission line structures which may have devastating economical and social consequences. In September 1996, Manitoba Hydro Company, Canada, reported that wind damages around ten million US dollars due to the failure of 19 power transmission lines (McCarthy and Melsness, 1996). Investigations of transmission line failures in Americas, Australia, South Africa and many other utility organizations have reported that more than 80% of the majority of all weather related line failures were the results of high intensity winds, ranging from fully mature tornadoes (Dempsey and White, 1996). Damages are caused by wind induced vibrations of conductors due to wind along or wind combined with an ice deposit or the weight load of the ice deposit alone. One of the main concerns to the power transmission is the wind turbulence-induced gust response which is giving rise to the high level dynamic loads, dramatically affects on power transmission lines. The geographical location of the line plays an important role to determine the risk of such events. For less exposed lines can also lead to the failure of the power transmission by fatigue of the different components of the line.

The main concern in the electric power industry is to accurately predict vibrations phenomena for more rational design of transmission line. It is believed that the accidents happen due to galloping although actual cause is unknown in majority of the causes. It is realized that galloping is a rare and an unpredictable event caused by interaction of wind and ice accretion in conductors. If either ice or wind is absent, galloping does not occur but when the both are present, galloping doesn't always result (Pasha, 1989). Therefore, interpretation of such response is difficult and sometimes, it may not depend on theoretical assumptions about which even experts may disagree (Rawlins, 1978). Some researchers investigated the vibration characteristics of bundle conductors transmission lines. Yamaguchi and Xie (1999) investigated the fundamental characteristics of galloping in bundle conductors transmission lines with numerical analysis and comparing the results with field measured data. Gurung *et al.* (2002), identified galloping as well as gust response of ice-accreted transmission lines based on field observed data analysis and separated the major galloping component from mixed mode of gust and galloping vibration. Their results show that there is a possibility of having large amplitude galloping together with gust response in vertical motion of ice-accreted transmission lines. Also, Gurung *et al.* (2003), identified and characterized galloping of transmission line based on multi-channel modal analysis by using field measured data. They proposed the method to identify galloping which are random decrement method (RDM) and eigensystem realization algorithm (ERA). Based on those modal parameters, galloping events were identified and performance of proposed method was tested by introducing usual buffeting analysis. Yamaguchi and Gurung (2005) characterized wind induced vibration by single-channel field data analysis based on piece wise application of Prony's method. Results showed some of events were identified as galloping, and most of events were gust responses which were confirmed partly by analytical buffeting analysis. In spite of this fact, there is usual tendency of paying attention to discuss galloping based on field data. To do so, there are possibilities of misinterpreting gust response as galloping. Presence of large amplitude gust response in transmission lines cannot be overlooked in gusty wind, which was pointed out by Ohkuma and Marukawa (1999). Keyhan *et al.* (2013) have been used gusty wind-transmission line conductor interactions model in surrounding moving air to investigate the dynamic interaction between wind and conductor motion. Miguel *et al.* (2012) presented the influence of extended pressure system wind effects on a transmission line response by means of numerical simulation. These computational methods are influencing of uncertainties in wind-force interaction on response prediction.

Therefore, in evaluating possible causes of such accidents and developing appropriate counter measures, it is important to have a clear interpretation of the nature of vibrations that actually occurs in the field. Usually large amplitude vibrations are interpreted based on field measured data such as time series, lissajous diagrams and power spectra. Some researchers also proposed some method and went through those methods to interpret field measured response. In this study, gust response analysis of transmission lines have been conducted based on developing three dimensional finite element (FE) model to interpret field measured wind induced vibrations. Gusty wind forces have been simulated from field measured wind characteristics data.

2.0 Outline of Overhead Transmission Lines

This study was conducted of two overhead transmission lines; both are bundle conductor type and due to geographical condition its cable profile are inclined. Detail geometric properties are given in Table 1. Spacer arrangement of both transmission lines are shown in Figure 1. Dead-end span data of transmission line–A are given, whose cable attached point difference at two ends is 40 m and the maximum sag is 35.1 m. In case of suspension span of transmission line–B, three spans maximum sags are 3.3 m, 10.26 m and 9.43 m respectively, those were measured at the time when temperature was -6°C.

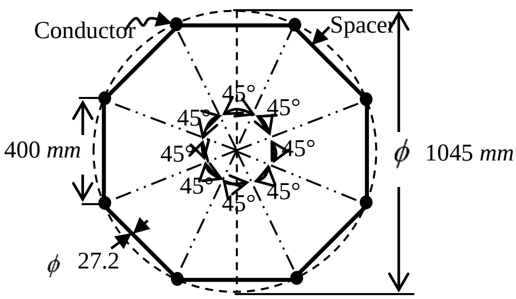

(a) Transmission line - A

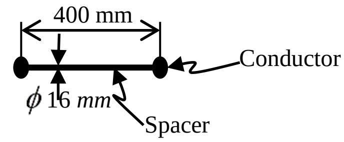

(b) Transmission line -B

Figure 1: Detailed of bundle conductors with spacers

Table 1 Geometric properties of two overhead transmission lines

Description	Transmission line-A	Transmission line-B
No. of conductors	8	2
No. of spans	1	3
Span length (m)	615	249, 439, 421
Sag to span ratio	0.057	0.013, 0.023, 0.022
Per single conductor unit mass(kg/m/conductor)	3.056	1.328
Conductor diameter (mm)	40.3	24.5
Conductor spacing (m)	0.40	0.40
Young's modulus of conductor (N/mm2)	69900	90600
No. of spacers	13	7, 10, 10
Spacer weight (kg)	28	6.7
Insulator length (m)	13.905	3.5
Insulator weight (kg)	14330	290

3.0 Field Measured Data Study

Field measured data analysis is necessary to predict the maximum vertical amplitude of wind-induced responses. It is essential to design the transmission line under the conditions of design wind velocity. The field-measured data is, however, lacking both in quality and in quantity, and their reliability is not necessarily high, while there is an advantage of directly dealing with one of the most important parameters in the design (American Society of Civil Engineers, 1990). But, it gives us the information of the nature and behaviour of vibrations that actually occur in the field. The field measured data used in this study are power company supplied data.

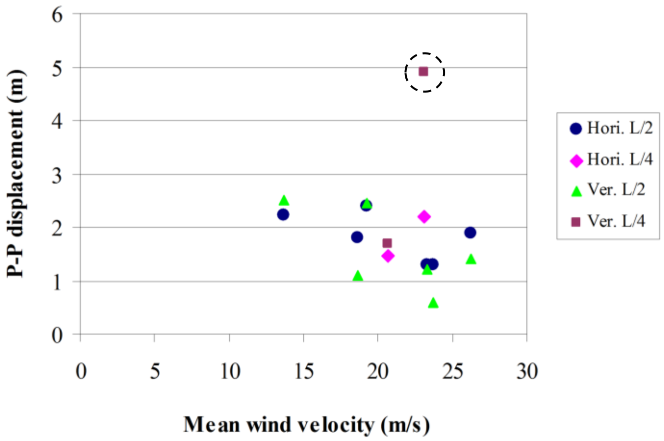

Figure 2: P-P displacements of transmission line-A

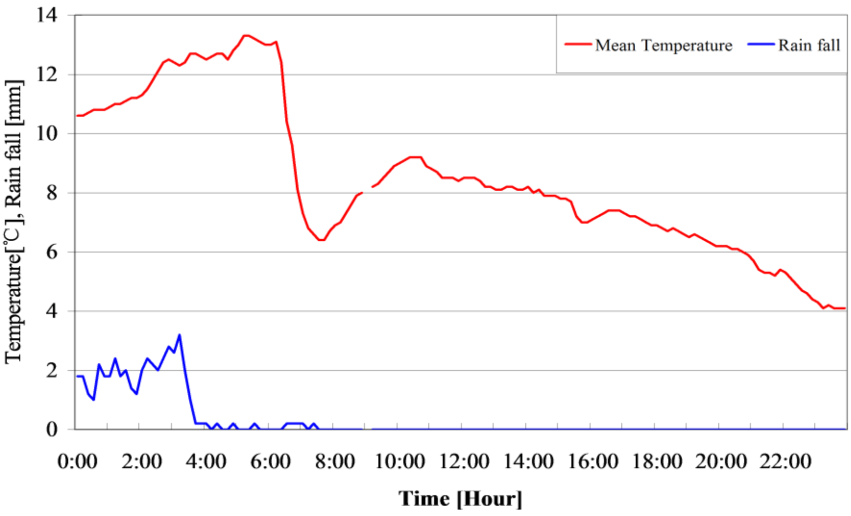

Figure 3: Meteorological data of whole day

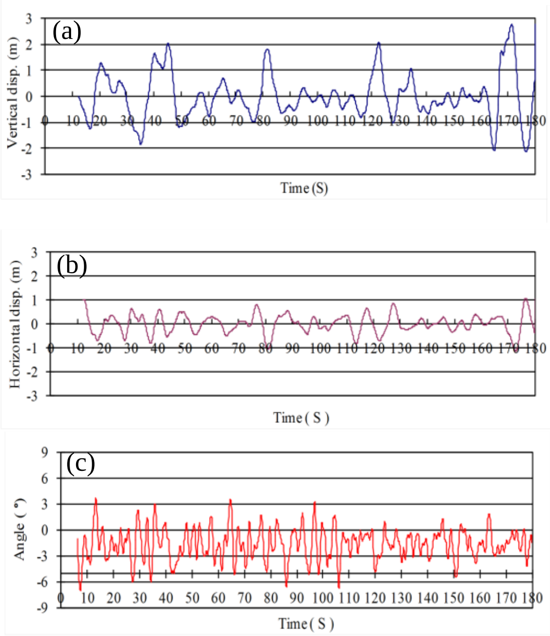

Figure 4: Time series displacements of line-A
(a) vertical (b) horizontal (c) torsional

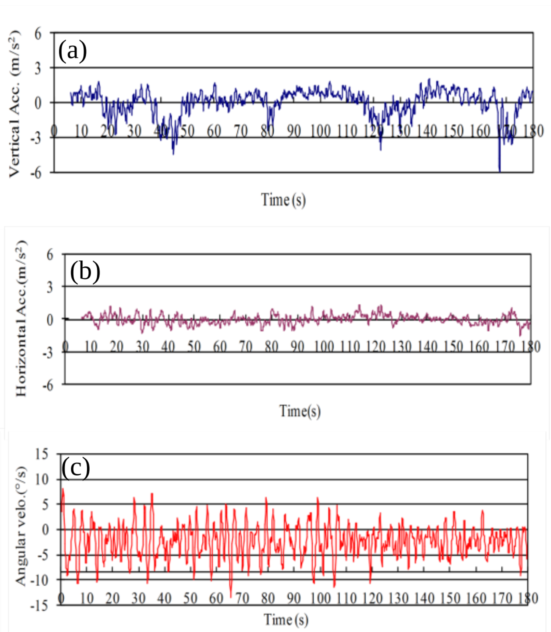

Figure 5: Time series accelerations of line-A
(a) vertical (b) horizontal (c) torsional

Wireless sensor was used to measure the vibration acceleration of the conductors in three directions. The wind and acceleration data were sampling in different frequencies. The 10 min average wind data and acceleration data are commonly practices that are used in this study. Time series displacements are obtained from acceleration data by writing some codes in excel sheet.

Figure 2 shows the peak-to-peak displacements of vertical and horizontal directions of transmission line - A. From this figure it can be observed that one peak-peak displacement is very large about 4.9 m. This maximum displacement is on vertical direction at quarter span, occurs at time 16:53, when mean wind velocity was 23.1 m/s. Also the temperature was 7.3°C in that time and there was no rain as well ice storm in that day shown in Figure 3. Time series displacements and accelerations at quarter span are shown in Figures 4 and 5 respectively. In case of vertical direction, it can be clearly shown that there are large amplitudes of displacements as well as accelerations that occur randomly. Other cases like horizontal and torsional displacements and time series accelerations are not occurring randomly. The Power Spectrum Density (PSD) of vertical, horizontal and torsional responses for maximum amplitude on time 16:53 are shown in Figure 6. The frequency obtained in vertical spectrum is very low which is less than 0.05 Hz and horizontal and torsional spectrum are quite different then the vertical case. Many peaks obtained in different frequencies in both horizontal and torsional cases. Also horizontal and torsional frequencies are coupling, that is, same frequency peak is obtained in both cases.

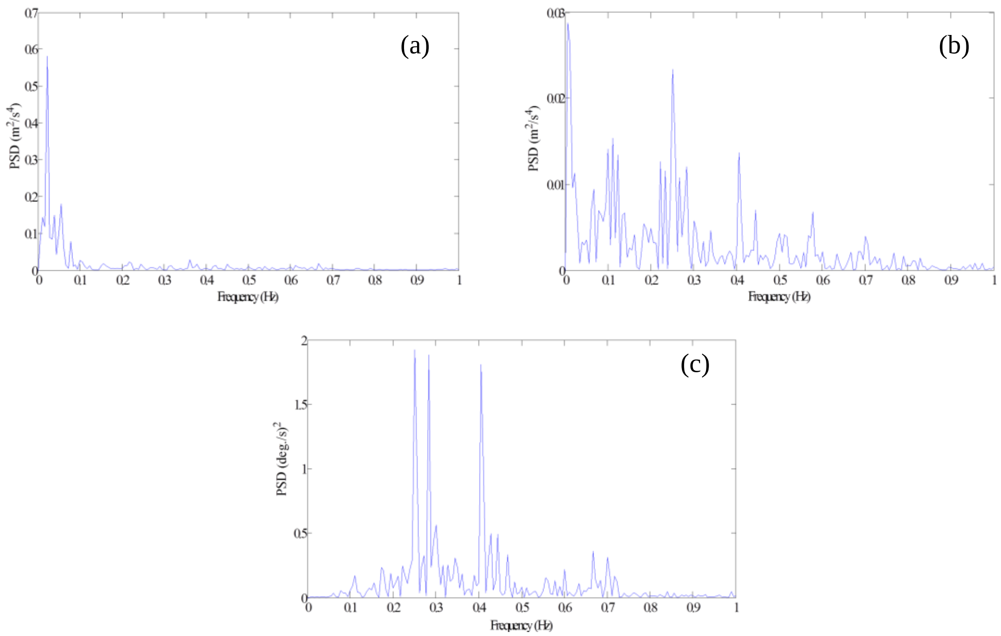

Figure 6: Power Spectrum Density of transmission line-A (a) Vertical (b) Horizontal (c) Torsional

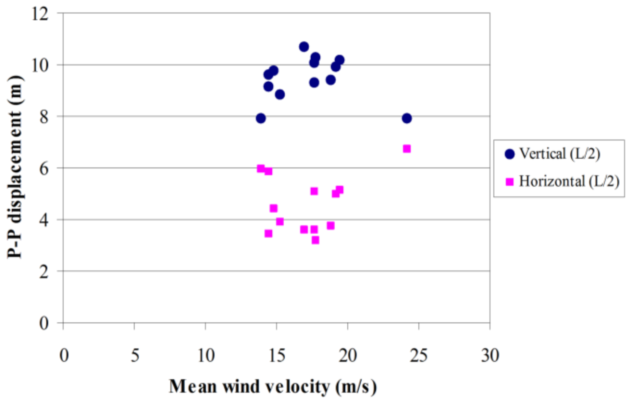

Figure 7: P-P displacements of transmission line-B

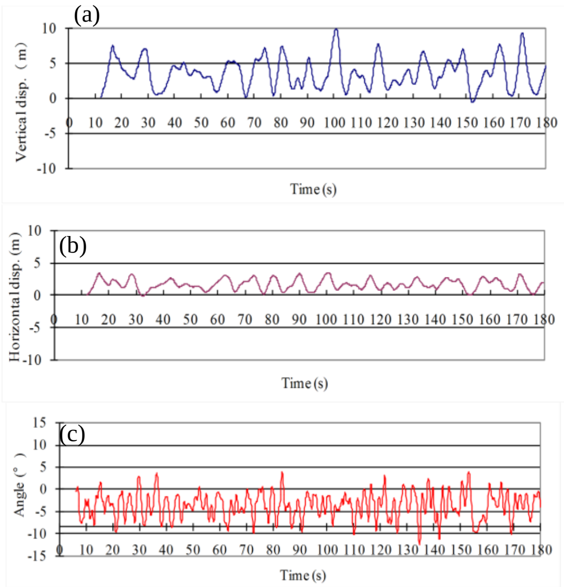

Figure 8: Time series displacements of line- B
(a) vertical (b) horizontal (c) torsional

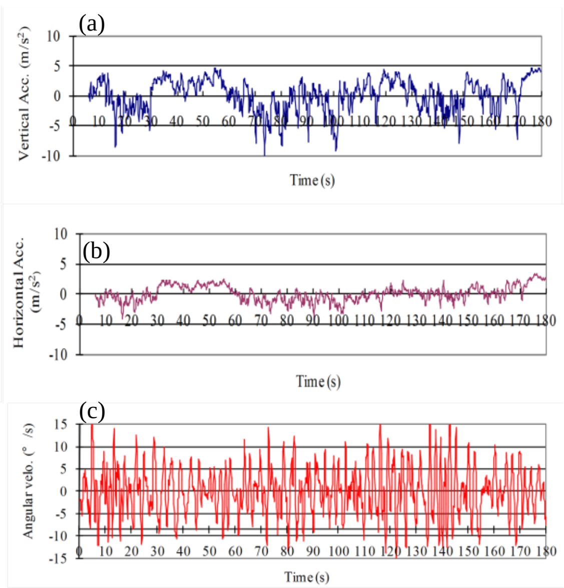

Figure 9: Time series accelerations of line- B
(a) vertical (b) horizontal (c) torsional

Peak-to-peak displacements of suspension span of transmission line-B are shown in Figure 7. There are several number of events occur when the peak-to-peak vertical displacements are between 9-10.5 m at midpoint of both spans. These large amplitude vibrations occur on different days and different times. After observing the different days meteorological data it can be seen that all days temperature is negative (-5°C ~ -10°C) and also rain occurs on those days. Therefore, there is a possibility of ice storm and ice accumulation on transmission line conductors on those days. Among those maximum displacements, one peak-to-peak highest vertical displacement is 10.69 m on times 20:55. In this case time series displacements and accelerations are shown in Figures 8 and 9 respectively. In case of vertical direction, there are large amplitudes of displacements as well as accelerations that occur randomly. Other cases like horizontal and torsional displacements and time series accelerations are not occurring randomly. Figure 10a shows the maximum spectrum peak frequency is very low, less than 0.05 Hz. Also there are two clear peaks in 0.19Hz and 0.28Hz. In the same time, maximum horizontal peak frequency also very low, besides this there are also two peaks in 0.28 Hz and 0.49 Hz, and torsional spectrum consists many peaks. After studying all events spectrum excluding the low frequency response, it is observed that in vertical case, 0.19 Hz and 0.28 Hz are mostly dominated and in horizontal case 0.17Hz, 0.28Hz and 0.49Hz are mostly dominated. In case of torsional vibration many peaks are observed between 0.24~0.6 Hz and some of them are coupling with horizontal.

According to the galloping theory, large amplitude galloping vibration occurs when ice storm occurs and usually bundle conductors galloping are self-excited modal response. In case of galloping response, vertical and torsional vibrations are coupling and negative damping occurs (Gurung *et al.*, 2003). Therefore, in transmission line-A, it is observed that maximum peak occurs in vertical direction for very low frequency and there is not any possibility of dynamic amplification due to resonance and this response component can be considered as a quasi-static response. That is, most of the energy of wind fluctuations is associated with low frequency component. From spectral analysis result,

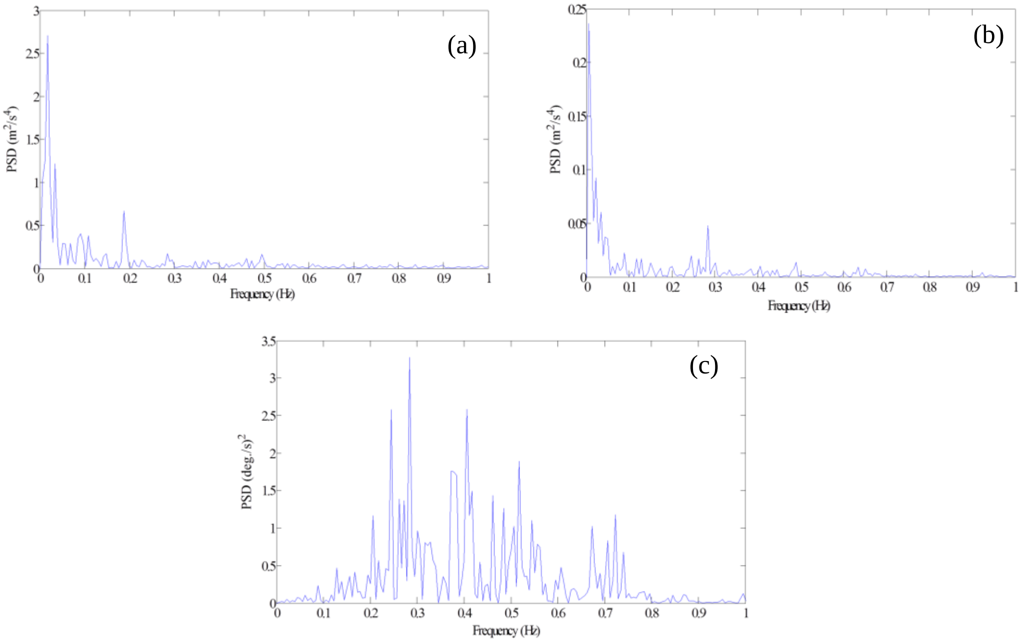

Figure 10: Power Spectrum Density of line-B (a) Vertical (b) Horizontal (c) Torsional

it is observed that vertical vibration are not coupled with torsional vibration but horizontal vibrations are coupled with torsional vibration. Also from meteorological data shown in Figure 3, there is no ice storm and no ices are accumulated on the conductor. Up to this discussion, it is understood that cause of large amplitude vibration that occurs in transmission line-A are not galloping. Also from time series data it is observed that displacement and acceleration are randomly occurred. That is, it is related to randomly fluctuated wind components. These types of peaks give us the information of how quickly change the velocity as well as displacement. Also acceleration is directly related to the inertia force. Inertia is a non-quantifiable property of matter by which it remains at rest or in uniform motion in the same straight line unless acted upon by some external forces which is similar to the behavior of gust response.

In case of suspension span of transmission line-B, it is seen that maximum peak shows in vertical direction, whose frequency is very low. Also there are two clear peaks in 0.19Hz and 0.28Hz in second span. Spectral analysis result also shows torsional dominant frequency are in high frequency between 0.24~0.6 Hz. Some of higher frequencies of vertical as well as horizontal directions are coupled with torsional frequency. Observing the different days meteorological data it is seen that all days temperatures are negative and also rain occur on those days. Therefore, possibility of ice storm and ice accumulation on transmission line conductors on those days. Also from time series displacement and acceleration datas, it is seen that some peaks occurs randomly, but other large peaks do not occur randomly. Up to this discussion, it can be understood that cause of large amplitude vibration of transmission line-B that occur in the field are due to mixed mode vibrations. Only for discussing field measured data, it is not possible to interpret the results accurately. For that reason, it is necessary to do the numerical analysis of these two transmission lines. Eigenvalue analysis is needed to check the resonance and also gust response analysis is needed to check the behaviors of gust response.

4.0 Eigenvalue Analysis of Transmission Lines

The usual first step to perform a dynamic analysis is determining natural frequencies and mode shapes of the structure with damping neglected. These results characterize the basic dynamic behavior of the structure and are indications of how the structure will respond to dynamic load (Blakey, 1993). The number of natural frequencies and associated mode shapes is equal to the number of degrees-of-freedom (DOF), that have mass or the number of dynamic DOF in a structure. Natural frequencies and mode shapes are functions of the structural properties and boundary conditions. Computation of the natural frequencies and mode shapes is performed by solving an eigenvalue problem. Here numerical analysis was done based on Finite Element (FE) analysis. This section is devoted to develop a FE model of transmission lines and finally eigenvalue analysis is done for checking dominant frequency and comparing those with field measured results.

4.1 Finite Element Model of Transmission Lines

Transmission lines were modeled by using commercially available ANSYS (2005) software. Conductors were modeled by PIPE59 element with rotation degree of freedom. This element has stress stiffening, large deflection capabilities and dynamic analysis is useful of this element. Insulators were modeled by BEAM4 element. Bundled conductor arrangements consists spacers to keep the distance between the sub conductors. Spacers were modeled by BEAM4 element and considering each spacer as a rigid body. So, the spacer possesses in general six DOFs. Also, connection between cable and insulator are considered as rigid body and boundary condition in both displacement and rotation in all directions are restrain. Transmission line-A is the bundle conductor transmission line which consists of 8 conductors. Span length of transmission line-A is 615 m, conductor attached point difference of this span is 40 m and sag is 35.1 m. FE modeled of transmission line-A is shown in Figure 11. In this model total number of elements used is 1098, total number of node is 972, and total number of DOF is 5832. Figure 12 shows the FE modeled of transmission line-B, which consists of 2 conductors. Conductor attached difference, sag, insulator and spacer are also shown in this figure. In this model total number of element used is 467, total number of node is 442, and total number of DOF is 2652.

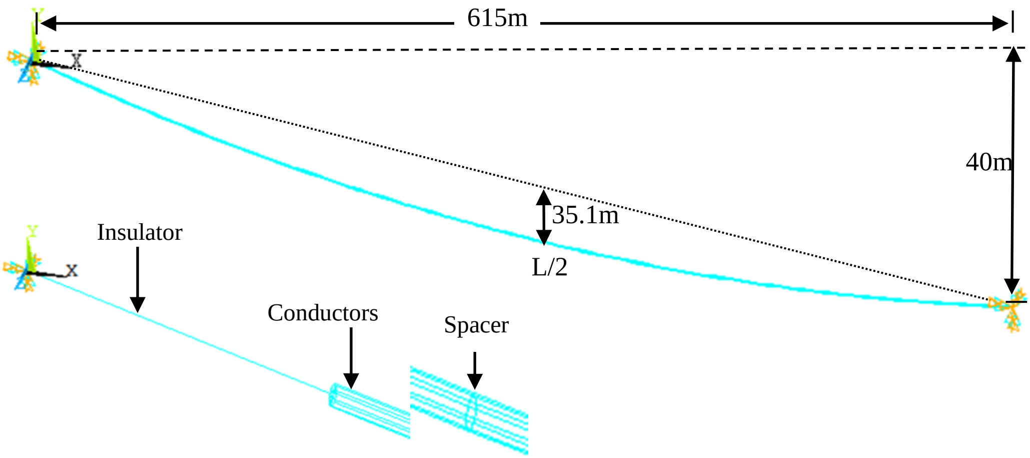

Figure 11: FE model of transmission line-A

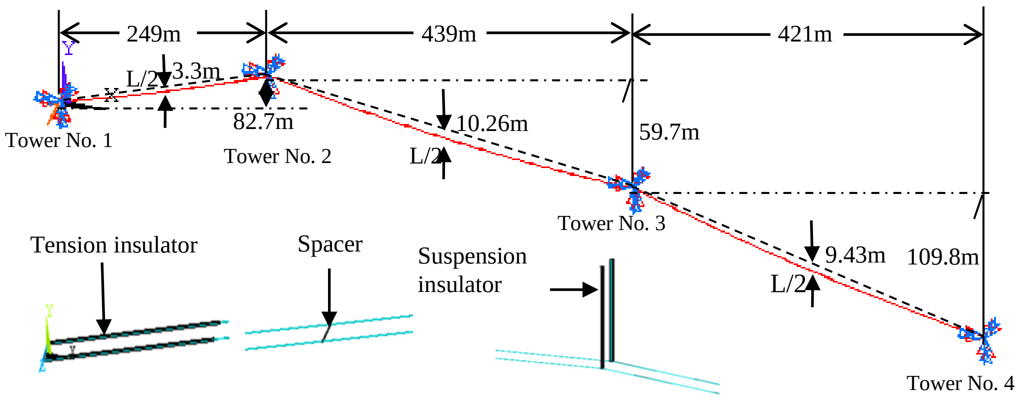

Figure 12: FE model of transmission line-B

4.2 Eigenvalue Analysis Results

The mode shapes and the natural frequencies of transmission line-A and B are shown in Figures 13 and 14 respectively. Each mode is symbolized by a letter indicating the kind of displacement (*H* = horizontal, *V* = vertical, *T* = torsional) and by a number giving the number of loops in the span (ie. 1, 2, 3 or 4). The subscripts *u-u*, *u-d*, *u-d-d*, *d-u-d* means up-up, up-down, up-down-down and down-up-down modes respectively. In case of multi span transmission line system with suspension insulator this type of modes will happen because of span length differences. From eigenvalue analysis result of transmission line-A, it is seen that first horizontal frequency is 0.099 Hz, however the first natural frequency on vertical direction is missed due to the initial sagging configuration of cable. Second horizontal as well as vertical natural frequencies are 0.197 Hz and 0.195 Hz respectively also third horizontal as well as vertical natural frequencies are 0.296 Hz and 0.279 Hz respectively. Also a pure torsional mode was found in 0.607 Hz. These eigenvalue analysis frequencies are comparing with dominant frequency from PSD of field measured responses. Clear peak of vertical response at quarter span on same days and time 18:27 occur when frequency is 0.1947 Hz and this response is resonant with 2nd vertical mode. Also, clear peak of horizontal response at mid span on same day and time 19:23 occur when frequency is 0.295 Hz and this response is resonant with 3rd horizontal mode.

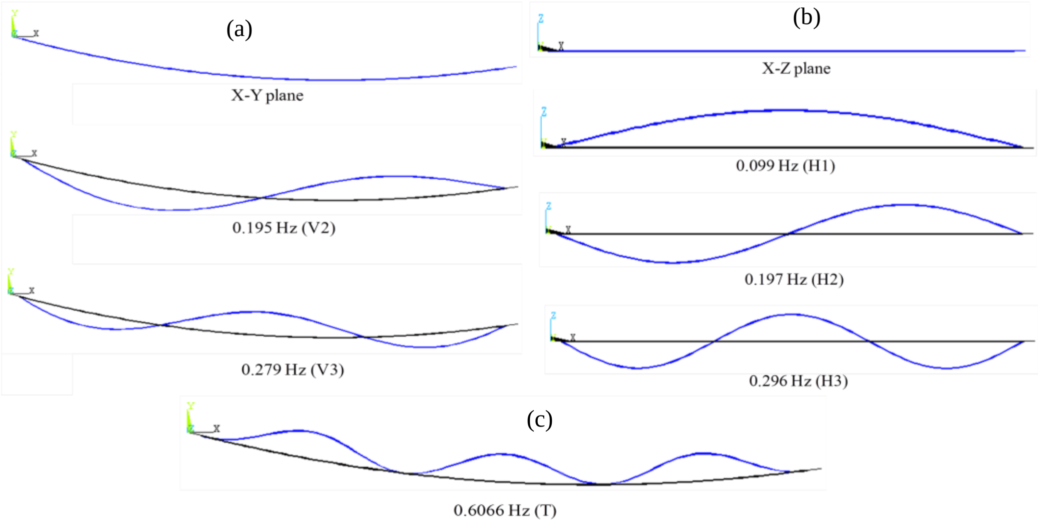

Figure 13: Eigenvalue analysis results of transmission line-A (a) Vertical mode (b) Horizontal mode (c) Torsional mode

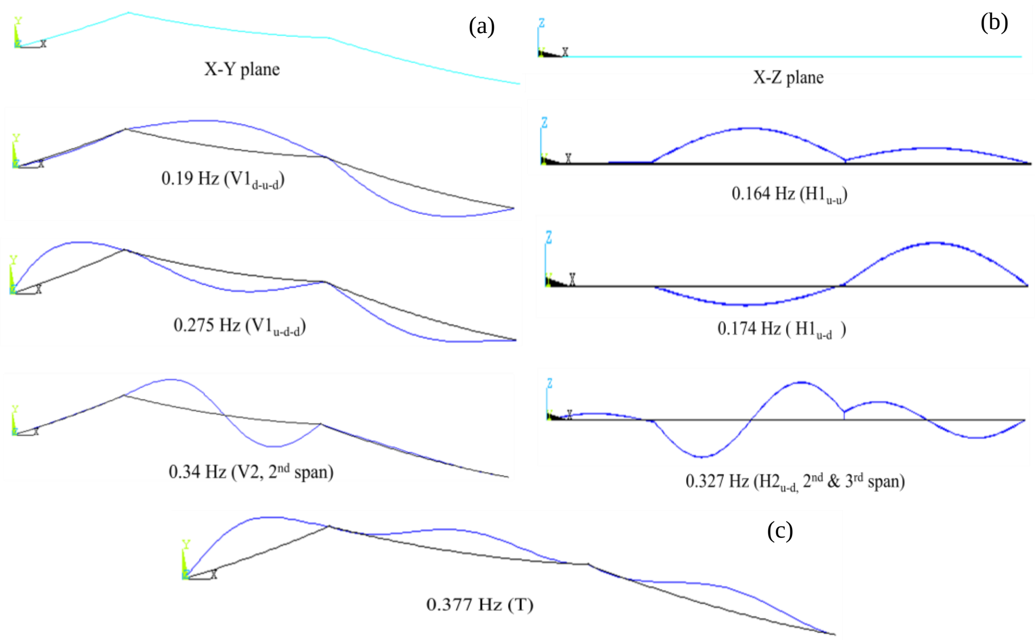

Figure 14: Eigenvalue analysis results of transmission line-B (a) Vertical mode (b) Horizontal mode (c) Torsional mode

Also from eigenvalue analysis result of transmission line-B, it is seen that there are up-up, up-down mode are obtained due to the multi span with different span length. In this case first horizontal up-up and up-down mode are obtained at 0.164 Hz and 0.174 Hz respectively, also first span first mode frequency is very high 0.288 Hz because of small span corresponding to others span. However the first natural frequencies of vertical direction on down-up-down and up-down-down modes are 0.19 Hz and 0.275 Hz respectively. Second horizontal mode occur in 2nd and 3rd span with the frequency of 0.327 Hz and in this time first span goes to first mode. Second vertical mode obtained in 2nd span when the frequency is 0.34 Hz as well as 3rd span 2nd vertical mode natural frequency is 0.35 Hz. Also pure torsional mode was found in 0.377 Hz.

Eigenvalue analysis results are comparing with dominant frequency from PSD of field measured responses. Clear peak of vertical response at quarter span on time 14:47 occur when frequency is 0.196 Hz and this response is resonant with first vertical down-up-down mode of transmission line-B. In this case there is also a clear peak on 0.35 Hz which is resonant with 2nd vertical mode on 3rd span. Clear peak of horizontal response at mid span on time 12:49 occur when frequency is 0.32 Hz and this response is resonant with 2nd horizontal up-down mode of 2nd and 3rd span. Beside this there are also some dominant frequencies of mid span as well as quarter span are resonant with natural frequencies of transmission line-B. But when maximum response occurs frequencies are not always resonant with natural frequencies of the transmission line-B. For example, when the maximum vertical amplitude (10.69 m) occurs, in that time maximum peak value frequency is very low, less than the natural frequency of transmission line-B, besides this there are also two clear peaks in 0.19 Hz and 0.28 Hz, which is resonant with natural frequency of the structure. So, the small frequency peak response will be happen due to quasi-steady gust force and it can be checked by gust response analysis.

5.0 Simulation of Turbulence Wind

Normally fluctuating considered Kaimal proposed spectrum (Ruoqiang *et al.*, 2012; Xuanyi *et al.*, 2013). Also in this study, both longitudinal and vertical fluctuating component are simulated by considering Kaimal proposed spectrum given in equations (1) and (2) respectively.

Longitudinal fluctuating component
$$\frac{f_n S_u(f_n)}{u_*^2} = \frac{200 f}{(1+50 f)^{\frac{5}{3}}} \quad (1)$$

Vertical fluctuating component
$$\frac{f_n S_w(f_n)}{u_*^2} = \frac{2f}{(1+5.3f)^{\frac{5}{3}}} \quad (2)$$

In which, the nondimensional quantity $f = \frac{f_n z}{\overline{U}(z)}$, and friction velocity is $u_* = \frac{k_c \overline{U}(z)}{\ln \frac{z}{z_0}}$,

Where, k_c is Karman constant and usually taken approximately as 0.4 (Simiu and Scanlan, 1996), $\overline{U}(z)$ is the mean wind velocity at elevation *z*, z_0 is the surface roughness. Mean wind velocity was taken by considering mean wind speed that actually happened in the field. Palmetto type surface roughness was considered and roughness coefficient is suggested by Simiu and Scanlan (1996).

Spectrums of both longitudinal and vertical directions are simulated from Kaimal proposed spectrum and then applying inverse Fourier transform to simulated spectrum to get the time series data of fluctuating components are shown in Figures 15 and 16. Longitudinal turbulence intensity of transmission line-A is ranged between 17-22% and transmission line-B is 15%. Here target longitudinal turbulence intensity is set as 20% for transmission line-A and 15% for transmission line-B. The vertical turbulence components are generally lower in magnitude than the corresponding longitudinal value. For well-developed boundary-layer winds, Holmes (2007) established a relation between longitudinal and vertical turbulence intensity. In which, vertical turbulence intensity is 55% of longitudinal turbulence intensity, which is considered in this study.

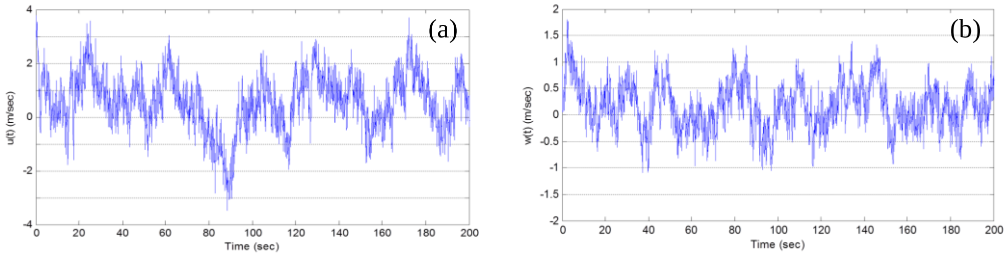

Figure 15: Fluctuating wind components of transmission line-A (a) Longitudinal (b) Vertical

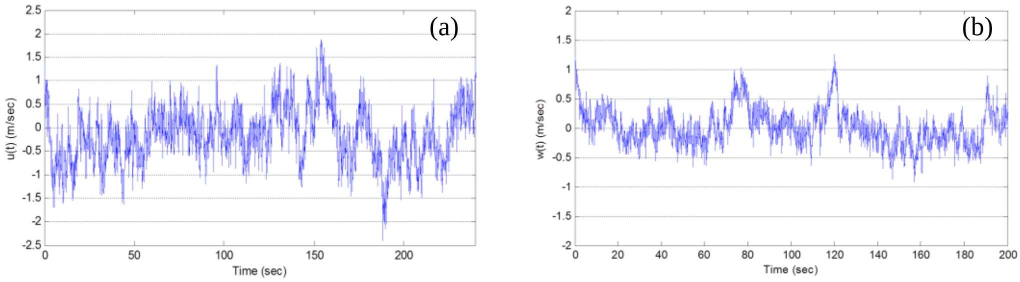

Figure 16: Fluctuating wind components of transmission line-B (a) Longitudinal (b) Vertical

6.0 Gust Response Analysis

6.1 Gust Forces on Transmission Line

As overhead transmission line is the flexible structure, therefore interactions between wind flow and conductor are most sensitive to wind-induced forces. In this study, self excited force is not considered; only moving by static force is considered. Wind flow develops local pressure over the body. The integration of these surface pressures over the body surface results in the centre of gravity of the cable cross section in a net force. The components of the force along wind and cross wind direction referred to the Figure 17 are as drag force F_D and lift force F_L. Because the circular cylindrical cross-section is only considered, there cannot be the aerodynamic moment for one conductor. According to Simiu & Scanlan (1996) and Holmes (2007), buffeting force acting on a conductor per unit length can be considered as;

$$F_D\ (t) = \frac{1}{2}\rho \bar{U}^2 D_c \mu \sin^2 \delta . [C_D \frac{2w(t)}{\bar{U}}]$$
$$F_L\ (t) = \frac{1}{2}\rho \bar{U}^2 D_c \mu \sin^2 \delta . [C_D \frac{v(t)}{\bar{U}}] \qquad (3a, b)$$

Where, ρ is air density, $\bar{U}$ is mean wind velocity, Dc is the conductor diameter, δ is horizontal angle of reference, C_D is drag force co-efficient which can be determined by

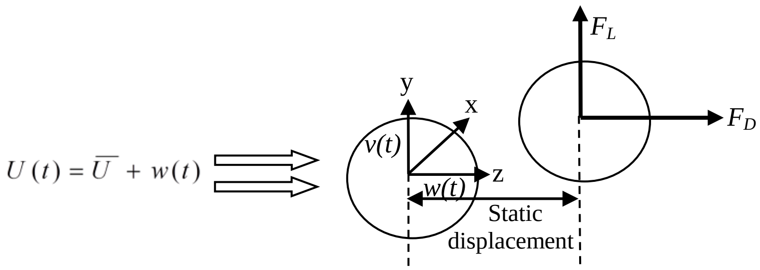

Figure 17: Section of a conductor subjected to wind force

Table 2: Parameter consideration value to calculate the gust force

Component	Value	
	Transmission line-A	Transmission line-B
C_D	0.77	0.9
ρ (kg/m^3)	1.218	1.218
$D_c\,(mm)$	40.3	24.5
$\bar{U}$ (m/s)	23	18
δ ($^\circ$)	25°	25°
μ	0.594	0.62

wind tunnel test. μ is the span reduction factor which is allows for the reduction in peak wind along the span of a conductor, due to non-simultaneous action of the gusts. Using equations (3a,b) and considering parameters value from Table 2, the gust forces are calculated.

6.2 Gust Responses

Static wind force was applied first to the transmission line at every node point and nonlinear analysis was conducted which gives certain displacement on both directions as well as rotation. Finally drag and lift forces were applied simultaneously at every node point of transmission line systems and obtained gust responses. Rayleigh damping (Clough and Penzien, 1993) is considered in this analysis.

Time series of gust responses at midpoint of transmission line-A are shown in Figure 18 and midpoint gust responses of tower no. 2-3 of transmission line-B are shown in Figure 19. From these figures it can be seen that vertical responses are larger than horizontal and torsional responses in both transmission line systems; this is because of gusty wind effect. The value of peak-to-peak vertical response of line-A is larger than the line-B. It is because of larger span length of line-A than the transmission line-B. However, the vertical response frequency of line-A is smaller than the line-B, because line-A consists 8 bundle conductors that is gravitational self weight and sag of line-A is larger than the transmission line-B. Also, the horizontal and torsional response frequency of line-A are larger than line-B, because of larger span length of transmission line-A.

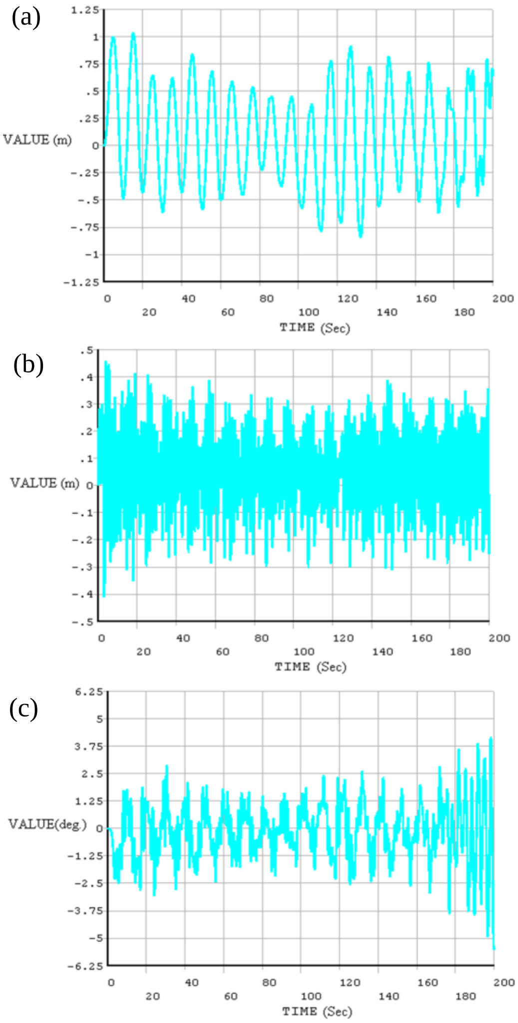

Figure 18: Responses at midpoint of line-A
(a) Vertical (b) Horizontal (c) Torsional

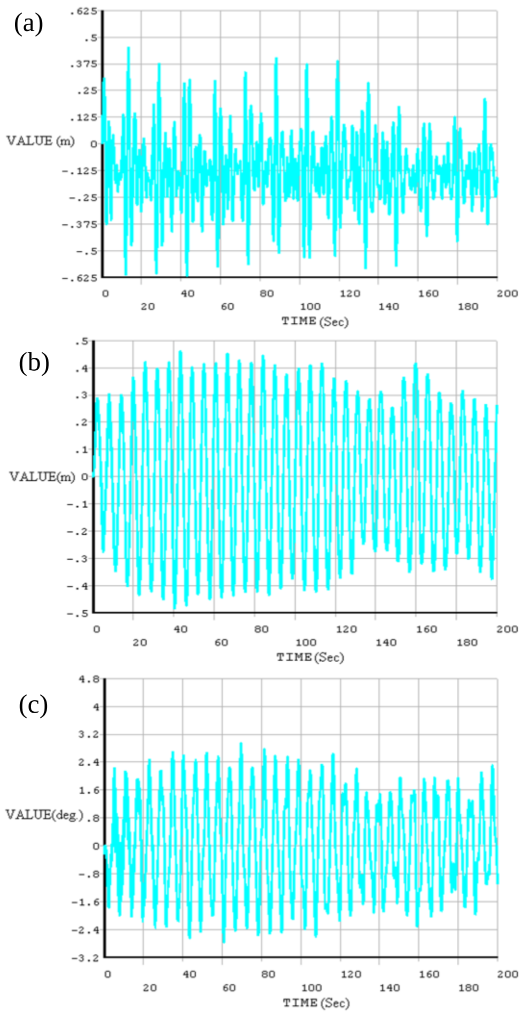

Figure 19: Responses at midpoint of line-B
(a) Vertical (b) Horizontal (c) Torsional

From the qualitative gust response results of both transmission lines, the behaviour of the gust response that occurs on transmission lines can be understood. In case of vertical response, it can be seen that how responses are changing dramatically due to the randomly fluctuate force components. Of course response value is dependent on the fluctuate components. The response behaviour that actually occurred in the field is discussed in section 3. Especially in vertical case, responses are fluctuated randomly and their magnitudes are changed dramatically. Which are similar behaviour to the numerically obtained gust responses. Therefore, large amplitude vibration that occurred in transmission lines can be occurred due to gust force, that is these responses will be gust response.

7.0 Conclusion

In this study, gust response analysis has been carried out by using finite element approach. To interpretation of the field measured response of transmission lines; three dimensional finite element models of transmission lines were developed. Eigenvalue analyses were carried out to observe the dynamic characteristics of the transmission lines. Gust forces were modeled by using field measured characteristics of wind. Finally gust response analyses were carried out and interpret the result with field measured responses. The following conclusion can be made from this study.

(i) Eigenvalue analysis results shows, suspension span with two bundle conductors line is more prone in torsional response than the dead-end span with eight bundle conductors line which is well confirmed with field measured response and gust response analysis results. Also from field measured data analysis and eigenvalue analysis results it can be conclude that large amplitude vibrations that occurred of transmission line-A are not due to resonant, but in transmission line-B, some large amplitude vibrations are found due to resonant and some are due to gusty wind.

(ii) In most cases, torsional motions are not in-phase with vertical vibrations and confirmed that causes of large amplitude vibrations are not due to galloping. Randomly peaks has been observed in time series acceleration which implies impulsive response and well confirmed with numerically obtained gust response analyses. However, some of events of transmission line-B, torsional motions are in-phase with vertical vibrations and there is a possibility of ice accumulation of conductors; therefore causes of these vibrations are galloping event.

Finally it can be concluded that due to gust forces large amplitude vibrations can occurs in transmission lines.

References

American Society of Civil Engineers (1990) Guidelines for transmission line structural loading, *ASCE manual and reports on engineering practice*. 74, ASCE New York.

ANSYS (2005) ANSYS release 10.0 documentations. ANSYS Inc., USA.

Blakey, K. (1993) MSC/NASTRAN Basic Dynamic Analysis User's Guide: version 68, MacNeal-Schwendler Corporation.

Clough, R.W. and Penzien, J. (1993) Dynamics of Structures, Second edition: McGraw-Hill Book Co., Inc., New York, USA.

Dempsey, D. and White, H. (1996) Winds wreak havoc on lines. *Transmission and Distribution World*, 48(6): 32-37.

Gurung, C.B., Yamaguchi, H. and Yukino, T. (2002) Identification of large amplitude wind-induced vibration of ice-accreted transmission lines based on field observed data. *Engineering Structures*, 24:179-188.

Gurung, C.B., Yamaguchi, H. and Yukino, T. (2003) Identification and characterization of galloping of Tsuruga test line based on multi-channel modal analysis of field data. *Journal of Wind Engineering & Industrial Aerodynamics*, 91:903-924.

Holmes, J.D. (2007) Wind loading of structures, Second edition, New York: Taylor & Francis.

Keyhan, H. McClure, G. and Habashi, W.G. (2013) Dynamic analysis of an overhead transmission line subject to gusty wind loading predicted by wind–conductor interaction. *Computers Structures*, 122:135–144.

McCarthy, P. and Melsness, M. (1996) Severe weather elements associated with September 5, 1996 hydro electric failures near Grosse Isle, Manitoba, Canada. *Manitoba Environmental Service Centre*, Environment Canada, 21.

Miguel, L.F.F, Riera, J.D., Joao, Kaminski, Menezes, R.C.R. (2012) Assessment of code recommendations through simulation of EPS wind loads along a segment of a transmission line. *Engineering Structures*, 43:1–11.

Ohkuma, T. and Marukawa, H. (1999) Galloping of overhead transmission lines in gusty wind. *First International Conference on Advance in Structural Engineering and Mechanics*, Seoul, Korea, 71-76.

Pasha, M.A. (1989) How to tame galloping of transmission conductors. *Electric world*, 203(7):43-46.

Rawlins, C.B. (1978) Transmission lines reference book: wind-induced conductor motion, Chapter 4- Galloping conductors, EPRI Res. Project 795, 113-168 pp.

Ruoqiang, F., Yan, G. and Jinming, G. (2012) Effects of high modes on the wind-induced response of super high-rise buildings. *Journal of Earthquake Engineering and Engineering Vibration*, 11(3): 427-434.

Simiu, E. and Scanlan, R.H. (1996) Wind Effects on Structures, New York: John Wiley & Sons.

Xuanyi, Z., Zhihui, H., Ming, G., An-an, Z., weiyu, Z. and Wei, F. (2013) Research on wind-induced responses of a large-scale membrane structure. *Journal of Earthquake Engineering and Engineering Vibration*, 12(2): 297-305.

Yamaguchi, H. and Gurung, C.B. (2005) Characterization of wind-induced vibrations in transmission lines by single-channel field data analysis. *Wind and structures*, 8(2):1-14.

Yamaguchi, H. and Xie, X. (1999) Galloping of overhead transmission lines with bundled multiple-conductors. *Proceeding of the 10th international conference of Wind Engineering*, Copenhagen/Denmark. 615-622.